An Optional Near-Infrared Camera for *Theia*

Rolf A. Jansen (ASU), Matt Beasley (U.Colorado - CASA)
Paul Scowen (ASU), Rogier Windhorst (ASU), Daniela Calzetti (U.Mass.-Amhurst)
James Rhoads (ASU), Sangeeta Malhotra (ASU), and the *SFC* Science Team.
April 21, 2009

In this section, we present preliminary specifications for and a strawman implementation of an additional Near-Infrared Camera (NIRC) for the *Theia* space telescope concept. *Theia* is a next generation UV–optical space telescope with a 4.00 m clear aperture, delivering diffraction-limited images at 300 nm, with three primary instruments — *XPC*, a camera that will operate in conjunction with an external occulter; *UVS*, a high-resolution ($R \gtrsim$ 30,000–60,000) far-UV spectrograph; and *SFC*, a wide-field, high-resolution mid-UV–near-IR (190–1075 nm) dichroic camera. The operational wavelength range of *Theia*'s instrument suite is presently limited at the long wavelength end by its Si-based detectors.

For most of *SFC*'s core science it would be valuable, and for particularly the cosmological programs it would be *highly* desirable to extend the present operational wavelength range for wide-field imaging with *Theia* further into the near-IR to $\sim$1950 nm. Here, we consider two options for a seperate Near-IR Camera covering the $\sim$900–1950 nm wavelength range. This camera shall be independent of and pose no additional restrictions on the designs of any of *Theia*'s other (primary) instruments (*XPC*,*SFC*, and *UVS*), shall not interfere with parallel operations of other instruments, and shall have an independent focus mechanism.

Scientific motivation for a Near-IR Camera

SFC will be a tremendous asset for wide-field studies of star formation regions and their relation to the surrounding environment, in both our own Galaxy, the Local Group, and other nearby galaxies. The early stages of star formation are, however, embedded within and obscured by dense clouds of molecular gas and associated dust. Even during the break-out stages, extinctions of several magnitudes may hamper our measurements of the physical processes of feedback to the ISM. One would wish to account for all young stellar objects that dominate such feedback. A significant fraction may be missed in an uncorrectible way in large-area surveys suffering from spatially variable extinction. Access to the near-IR, with extinctions that are 5–10 times lower than in the visible, would largely solve such issues.

Furthermore, while *SFC* will be a uniquely powerful instrument for wide-field cosmological studies to redshifts of up to $z \simeq 7.4$, an additional Near-IR Camera would make the *Theia* mission concept much more interesting for high-redshift studies that aim to penetrate the era of Cosmic Dawn – the first luminous objects in the universe (Pop III stars) and the subsequent onset of Pop II star formation and the condensation of the first globular clusters and sub-galactic $\sim$kpc-sized objects. The *WMAP* year 5 result demonstrates that the peak of cosmic reionization occurred at z=10.8$\pm$1.4, inaccessible to *SFC*. *JWST* can readily access the relevant wavelength regime, but will be able to search for $z \gtrsim 8$ objects over only small fields ($\sim$0.1 deg^2), and for wavelengths shorter than 2 μm it lacks both a suitable medium-band filter set and grisms. The high value of grism surveys has been demonstrated in recent years by surveys with *HST* for Lyα-emitters and other emission-line objects at intermediate and high redshifts.

We note that a wide-field Near-IR Camera on *Theia* does *not* compete with *JWST*'s capabilities, but rather complements them, since the Near-IR Camera would probe a very much different area in the parameter space characterized by $A \cdot \Omega \cdot \Delta \log(\lambda) \cdot \theta^{-1}$, where A denotes the telescopes primary aperture, Ω its instantaneous field of view (solid angle), $\Delta \log(\lambda)$ its wavelength agility (operational wavelength range, possibly multiplexed as in the case of *SFC*), and θ the angular resolution attainable. The Near-IR Camera could survey large areas of sky in order to *find* rare objects. *JWST* and next generation ground-based near-IR AO facilities will be available for detailed follow-up.

Design considerations and specifications for a Near-IR Camera

One of the key near-IR star formation tracers is the Paα emission line at 1875 nm. Together with mid- or

far-IR tracers of heated dust (e.g., 24 μm continuum emission), Paα can be used to account for the vast majority of ionizing photons emitted by young, massive stars in a star formation region, and do so in a more straightforward way than Hα. We will therefore require that Paα will be well blueward of the long wavelength cut-off of the Near-IR Camera. We wish, however, to mitigate the amount of thermal radiation outside the operational wavelength range. At the short wavelength end, we would wish to have some overlap with the *SFC* Red-Channel and offer an efficient filter centered near $\sim$950 nm that is not determined by the QE of the detector, but by the filter itself. We will therefore assume an operational wavelength range of 900–1950 nm and consider two options to cover it. First, a single-channel Near-IR Camera covering the entire 900–1950 nm wavelength range. Second, following the design choices of *SFC*, a dual-channel camera with a dichroic split at 1338 nm, just redward of the 1250 nm (*J*) broad-band filter.

Any core science program will need to be able to reconstruct the point spread function (PSF) delivered by the 4.00 m *Theia* OTA, which will produce diffraction-limited performance at all wavelengths $\lambda \geq 300$ nm. The Nyquist criterion from information theory dictates a cadence of $>$2 independent samples per resolution element. For a diffraction-limited PSF, the first Airy minimum occurs at $\theta = 1.22 \cdot \lambda/D$ and the FWHM of the core will be $\theta' = 1.03 \cdot \lambda/D$. In case of the Near-IR Camera, the *Theia* OTA will deliver diffraction limited images over the entire operational range. At the blue end of this range, at $\sim$900 nm, $\theta \sim 0.0566$ arcsec, implying that Nyquist sampling requires pixels of $\sim$0.0283 arcsec. Striking a compromise similar to that resulting from the *SFC* design study, we would rely on sub-pixel dithering and PSF reconstruction techniques to recover the diffraction-limited PSF. Dithering would be necessary in any case to fill the gaps between individual detectors in the FPA. Such techniques break down when the pixel sampling is coarser than 1 pixel per resolution element θ. The requirement of 1 pixel per FWHM at the blue end (900 nm) of the Near-IR Camera's operational wavelength range then dictates pixels no larger than 0.0566 arcsec.

We wish to cover an instantaneous field of view (FoV) that is identical in size and orientation to *SFC*'s Blue and Red Channels but, due to the seperate pick-off in the focal plane, offset therefrom on the sky. Assuming 2048$\times$2048 HgCdTe detectors (similar to, e.g., Hawaii 2RG detectors) with 18$\times$18 μm pixels, we could cover 19$'\times$15$'$ with 10$\times$8 detectors. Such a FPA would then measure $\sim$37.5$\times$29.9 cm, assuming $\sim$35 pixel interdetector gaps — less than $^1/_4$ the physical size of the *SFC* FPAs and containing 10$\times$ fewer pixels, allowing a far more compact design. In the case of a dual-channel implementation, we would have two such near-IR focal plane arrays. The Near-IR Camera's detectors would be passively cooled to 120 K and are assumed to be overcoated or equipped with a red-blocking filter with $>$96% transmission at $\lambda \leq$1900 nm, 50% transmission at $\lambda \sim$1950 nm, and $\ll$1% at $\lambda >$2000 nm.

The Near-IR Camera will require a Fast Steering Mirror (FSM) that allows pointing control to better than $^1/_4$ of a pixel (goal: $^1/_6$) and dither offsets and spacecraft drift correction independent of the spacecraft to an accuracy better than $^1/_4$ of a pixel over distances of a few pixels, and dither offsets accurate to better than $^1/_2$ of a pixel over distances of up to $\sim$100 pixels. All core science survey programs shall be built using one or more repetitions of a basic Observing Block of a dither pattern involving 3 'major' dither positions, offset from one another over a sufficiently large, non-integer number of pixels that the interdetector gaps are filled, and involving 3 sub-pixel 'minor' dithers at each such 'major' position to recover the PSF and reject cosmic ray induced signals (the latter depending on the detector read-out mode, e.g., direct integration versus up-the-ramp sampling).

The Near-IR Camera shall accomodate a minimum of 22 filters and 2 grisms. In the case of a single-channel implementation, this likely requires a 4- or 5-wheel assembly, preceded by a wheel containing a shutter and a diffusor. In the case of a dual-channel implementation, we baseline 12 filters + a grism in the Short-Wavelength Channel (SWC) and at least 10 filters and a grism in the Long-Wavelength Channel (LWC). This would likely require a 3-wheel assembly in the SWC and a 2-wheel assembly in the LWC, each preceded by a wheel containing a shutter and a diffusor. Thanks to the use of highly reflective Ag-coated optics within the Near-IR Camera, the optical design is far more flexible than that of *SFC*, and we anticipate that the filter sizes will be significantly smaller. The Near-IR Camera's overall throughput, its filter complement and the properties thereof shall closely resemble those identified in Table 1 and graphically represented in Figures 1 and 2. The Near-IR Camera shall have an internal illumination source to provide on-orbit flat-field calibration (via the diffusor).

In figures 3–5, a straw-man optical design is outlined for a single-channel implementation of a Near-IR

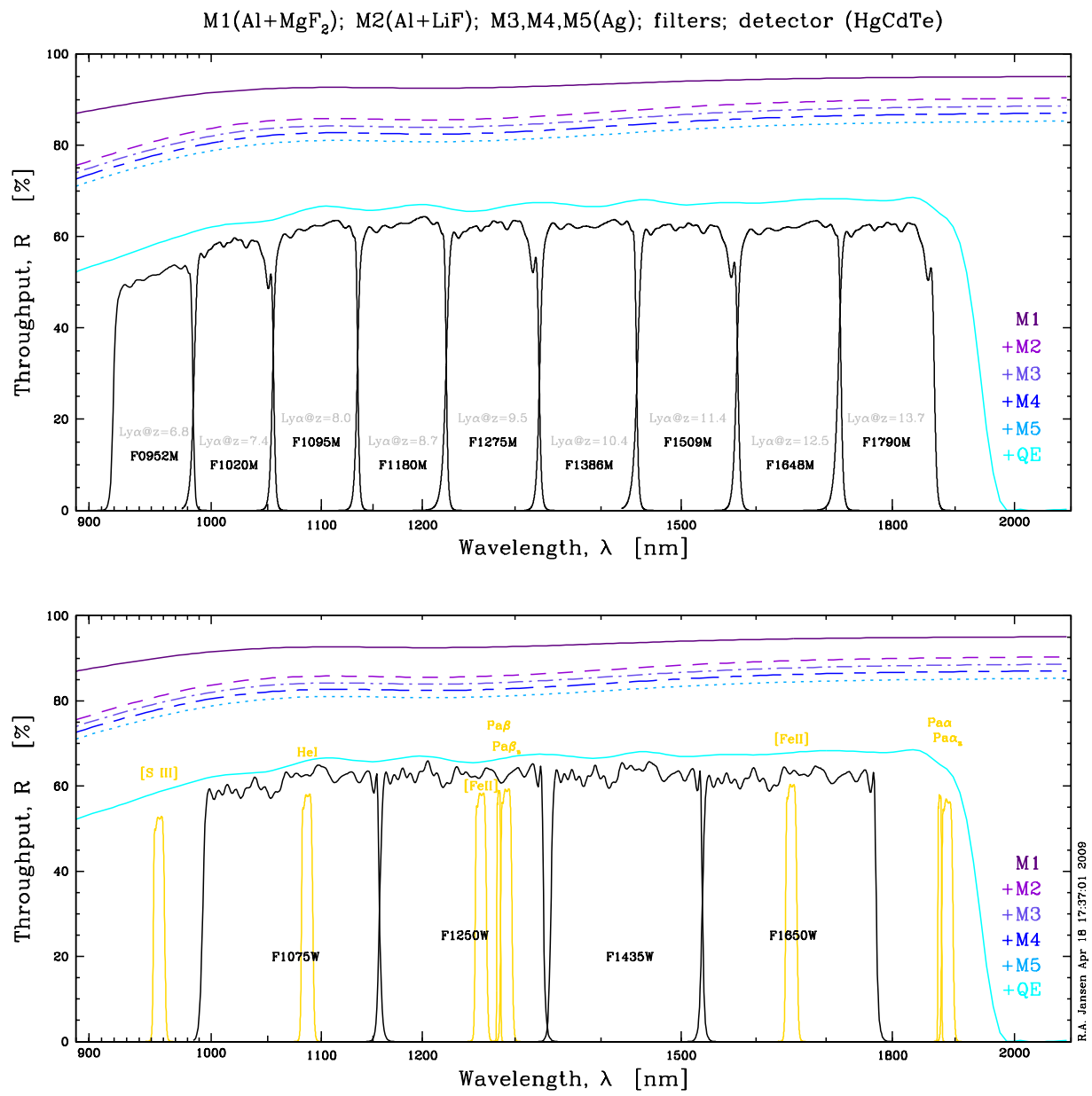

Fig. 1 — Projected Near-IR Camera overall throughput and the cumulative contributions to that throughput of each of the optical components in case of a *single-channel* implementation. All reflective surfaces internal to the NIR Camera are assumed to be overcoated with protected silver.

Camera for *Theia*, including a preliminary analysis of its anticipated optical performance, showing that the image quality is dominated by the 4.0 m primary with only marginal contributions from the camera design, and showing over 85% encircled energy within a radius of 18 μm.

Lastly, Table 2 gives an overview of the requirements and preliminary characteristics of each of the two implementations of a Near-IR Camera for *Theia*. The anticipated data volume from the Near-IR Camera in case of the dual-channel implementation could conceivably be up to 30% of that expected to be generated by *SFC* (assuming average individual exposure times as short as 60 s and 24 hr continuous operation — this is a strong upper limit to any actual use of the Near-IR Camera). For programs that require such intensive use of the Near-IR Camera, we would expect that *SFC* would *not* be available full-time for operation in

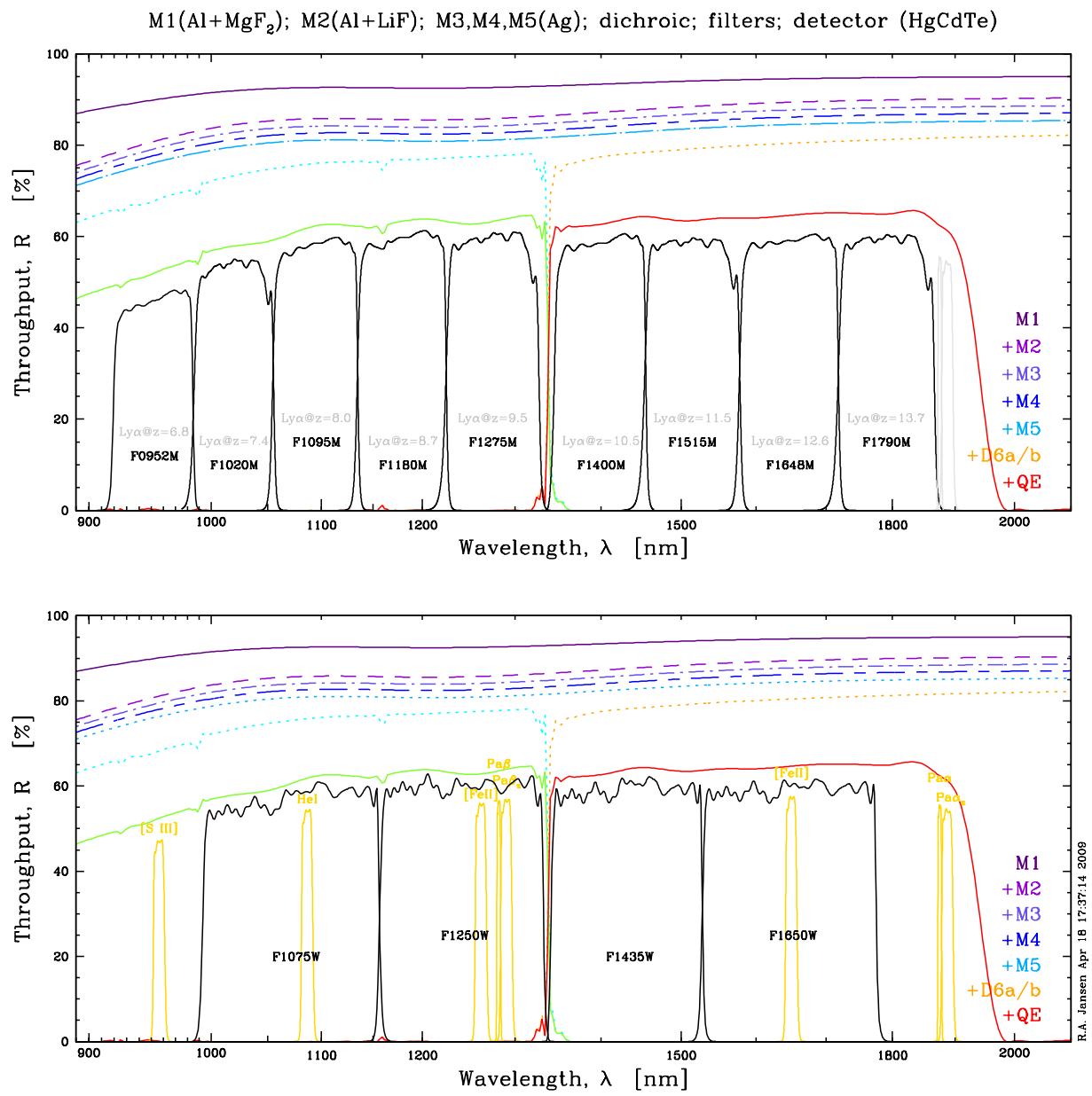

Fig. 2 — Projected Near-IR Camera overall throughput and the cumulative contributions to that throughput of each of the optical components in case of a *dual-channel* implementation with a dichroic split between the Short-Wavelength Channel and Long-Wavelength Channel at 1338 nm. All reflective surfaces internal to the NIR Camera are assumed to be overcoated with protected silver.

parallel. Similarly, during particularly intense survey-mode observing campaigns with *SFC*, the Near-IR Camera might not be available for parallel operations. However, depending on the typical exposure times of the active *SFC* observing program, we would anticipate that there would be many opportunities where both instruments would be able to be scheduled and usefully operated in parallel. For example, the anticipated data rate from *SFC* during (ultra-)deep cosmological surveys will have typical exposure times of 1000–2000 s, allowing simultaneous observations to be scheduled with a Near-IR Camera with almost arbitrary exposure times, without violating the maximum daily data rate of $<$6–7 Terabytes.

Table 1 — Near-IR Camera filter complement.*

Single-channel option:

Broad-band:							**Grism:**	
F1075W	F1250W	F1435W	F1650W				G1120L	G1625L
...	*J*	...	*H*				...	...
1075.9	1245.0	1435.3	1652.0				1120.0	1625.0
163.0	176.0	187.0	248.0				440.0	570.0
100.2	110.3	117.5	153.9				...	...

Medium-band:								
F0952M	F1020M	F1095M	F1180M	F1275M	F1386M	F1509M	F1648M	F1790M
Ly$\alpha_{z\sim6.8}$	*Y/Ly*$\alpha_{z\sim7.4}$	*Ly*$\alpha_{z\sim8.0}$	*Ly*$\alpha_{z\sim8.7}$	*Ly*$\alpha_{z\sim9.5}$	*Ly*$\alpha_{z\sim10.4}$	*Ly*$\alpha_{z\sim11.4}$	*Ly*$\alpha_{z\sim12.5}$	*Ly*$\alpha_{z\sim13.7}$
952.6	1020.2	1095.3	1180.2	1275.5	1385.9	1509.0	1648.2	1790.9
65.0	70.0	80.2	90.3	102.1	115.6	130.7	148.0	148.0
33.6	40.5	49.6	56.7	63.1	72.4	80.3	91.9	91.0

Narrow-band:								
F0956N	F1086N	F1262N	F1282N	F1290N	F1649N	F1875N	F1887N	
[S III]	He I	[Fe II]	Paβ	Paβ_z	[Fe II]	Paα	Paα_z	
956.3	1086.6	1262.3	1281.8	1290.3	1649.8	1875.1	1887.5	
9.4	10.6	12.4	4.2	12.6	16.3	6.2	18.4	
5.0	6.2	7.3	2.5	7.5	9.8	3.6	10.6	

Dual-channel (dichroic) option:

Broad-band:							**Grism:**	
F1075W	F1250W	F1435W	F1650W				G1120L	G1625L
...	*J*	...	*H*				...	...
1076.3	1245.0	1435.4	1652.4				1120.0	1625.0
163.0	176.0	186.0	248.0				440.0	570.0
93.5	105.0	110.7	146.6				...	...

Medium-band:								
F0952M	F1020M	F1095M	F1180M	F1275M	F1400M	F1515M	F1648M	F1790M
Ly$\alpha_{z\sim6.8}$	*Y/Ly*$\alpha_{z\sim7.4}$	*Ly*$\alpha_{z\sim8.0}$	*Ly*$\alpha_{z\sim8.7}$	*Ly*$\alpha_{z\sim9.5}$	*Ly*$\alpha_{z\sim10.5}$	*Ly*$\alpha_{z\sim11.5}$	*Ly*$\alpha_{z\sim12.6}$	*Ly*$\alpha_{z\sim13.7}$
952.6	1020.4	1095.4	1180.3	1275.4	1400.5	1515.0	1648.3	1791.0
65.0	69.9	80.1	90.3	102.0	110.2	124.1	140.5	148.0
30.0	37.2	46.6	53.7	60.4	64.9	72.3	83.1	87.1

Narrow-band:								
F0956N	F1086N	F1262N	F1282N	F1290N	F1649N	F1875N	F1887N	
[S III]	He I	[Fe II]	Paβ	Paβ_z	[Fe II]	Paα	Paα_z	
956.3	1086.6	1262.3	1281.8	1290.3	1649.8	1875.1	1887.5	
9.4	10.6	12.4	4.2	12.6	16.3	6.2	18.4	
4.5	5.8	7.0	2.4	7.2	9.4	3.5	10.1	

*For each filter, the five rows list the filter name, an alias or feature the filter aims to capture, the central wavelength (in nm), the FWHM in nm, and the Equivalent Width in nm. Most narrow-band filters must be sufficiently wide to accomodate relative velocities with respect to the Sun of at least -300 to $+2300\,\mathrm{km\,s^{-1}}$ (FWHM corresponding to $-500 < cz < +2500\,\mathrm{km\,s^{-1}}$), but the Pa$\alpha$ and Paβ filters designed for Galactic and Local Group surveys are narrower ($-500 < cz < +500\,\mathrm{km\,s^{-1}}$). The Pa$\alpha_z$ and Paβ_z filters should capture redshifted emission with $+500$ to $+3500\,\mathrm{km\,s^{-1}}$ and can serve also as continuum filters. Several of the medium-band filters, designed for cosmological work, also double as efficient continuum filters for the emission-line filters.

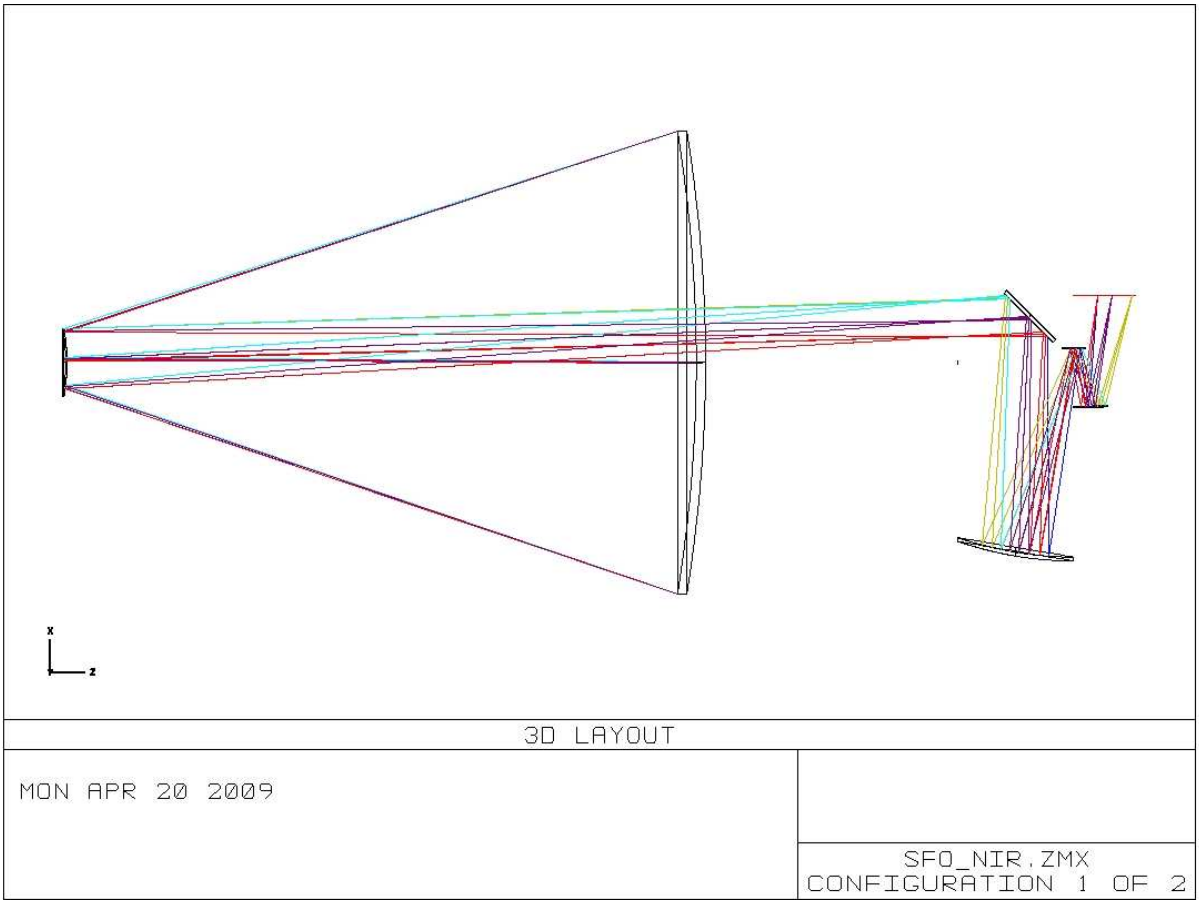

Fig. 3 — NIR Camera optical design (single-channel implementation), involving a total of six bounces.

Most likely descope path for this upscope

As discussed in the 'Descope Options' section for *SFC*, reduction of the Field of View is one of the worst descopes possible, undermining the goal of cosmological surveys for high-redshift objects with surface densities below 1/deg^2, and hence undermining the very mission of the near-IR camera.

A possible descope, affecting mostly the performance of the Near-IR Camera at the blue end of its operational wavelength range, would be to change the sampling criterion to 1 pixel per FWHM at the mid-point of that range, i.e., at 1400 nm instead of at 900 nm. This would allow covering the $19' \times 15'$ FoV with a smaller FPA array of only 7×5 instead of 10×8 HgCdTe detectors.

Pros:

• Cost savings of $\sim$\$50M or twice this for the dual-channel implementation ($\sim 2.3\times$ smaller number of detectors to fabricate and test to flight readiness level);
• Mass savings (reduction of the number of detectors and associated electronics; reduction in size of the FPA support structure);
• Power savings of $\sim$60–80W or twice this for the dual-channel implementation (reduction of FPA cooling and read-out);
• Reduction of the size of the radiator and heat-pipes, thermal shielding and baffles;
• Reduction by a factor of ~ 2.3 of the data volume that would need to be downlinked, and corresponding increase in opportunities for observations in parallel to *SFC*.

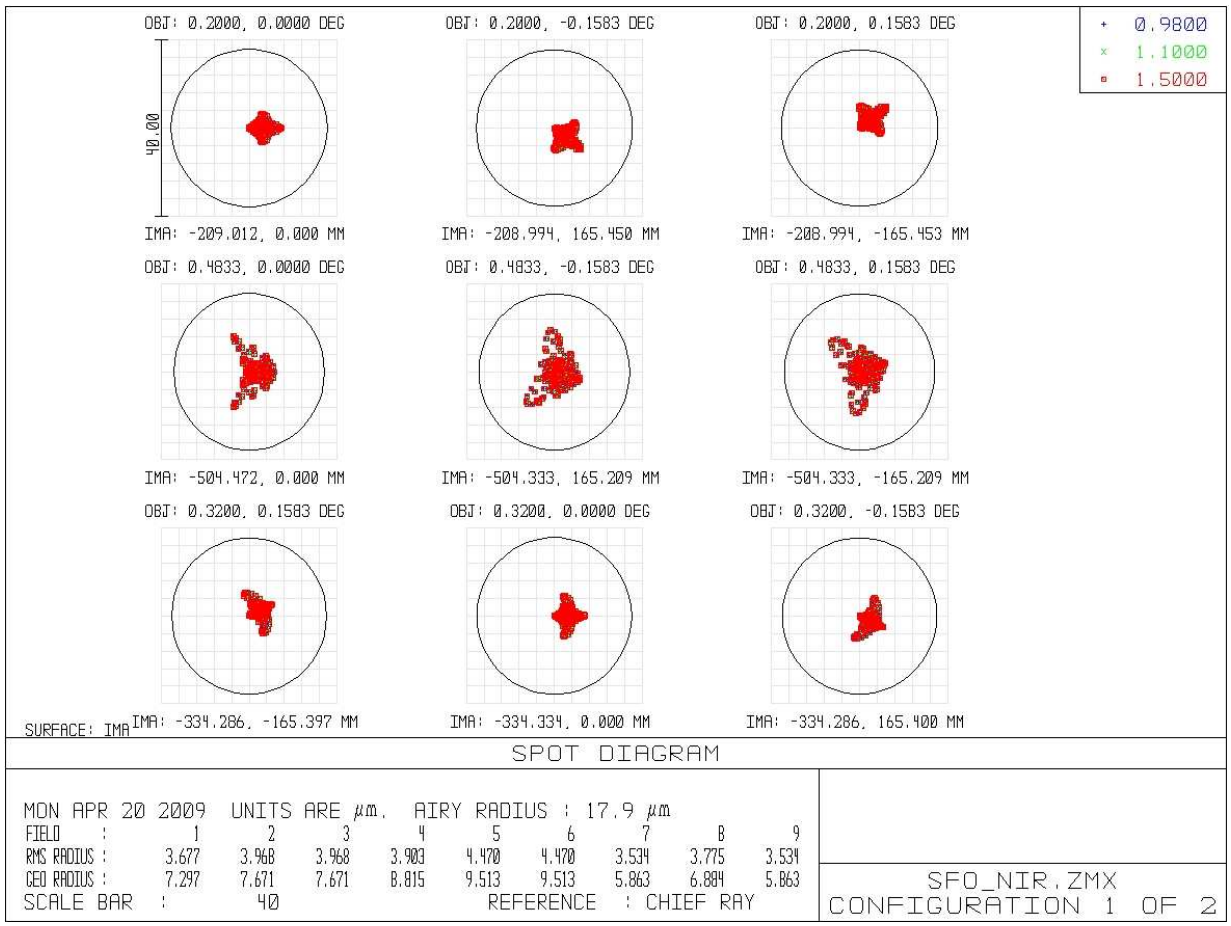

Fig. 4 — NIR Camera matrix spot diagrams as a function of position on the Focal Plane Array. Accross the entire $\sim 19' \times 15'$ FPA, the PSF is dominated by the 4.0 m primary mirror with only marginal contributions from the camera design.

Cons:

• The criterion of 1 instead of >2 pixels per FWHM (as required for Nyquist sampling), was already a compromise that was struck since the PSF was judged to still be recoverable through sub-pixel dithering;

• At the blue end, the PSF is likely to become only partially recoverable through the standard dithering strategy, leaving field-dependent PSF-variations and artefacts, negatively affecting both photometricity of the data and accurate centroiding for proper motions;

• Observing efficiency will be negatively impacted for programs that require the bluer filters and would require more elaborate dithering in order to recover the PSF;

• Sub-standard performance for a NASA flagship-class observatory in a wavelength range where there really isn't any technical difficulty to deliver diffraction-limited data.

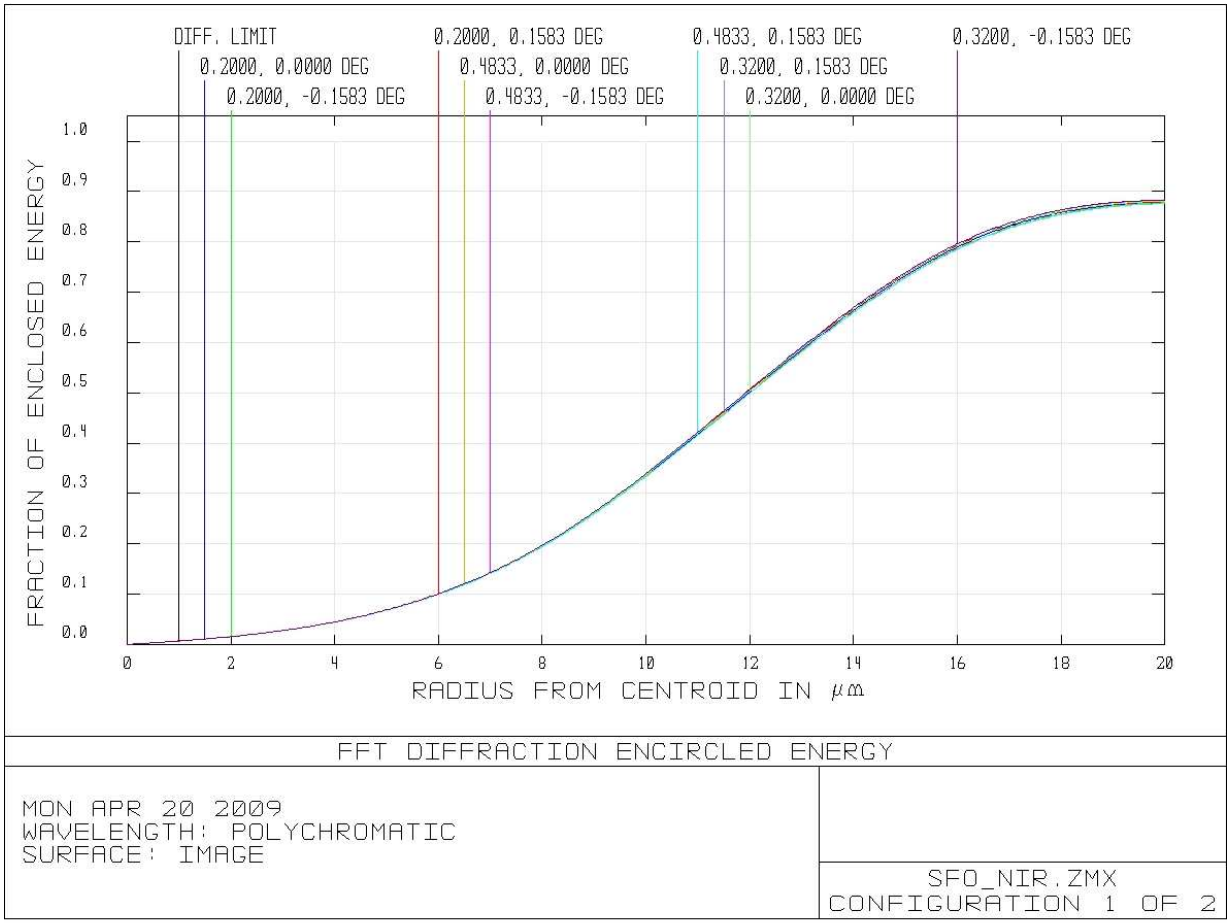

Fig. 5 — NIR Camera performance in terms of the enclosed energy as a function of centroid distance for a point source stimulus, showing $\gtrsim$85% encircled energy within a radius of 18 μm.

Table 2 — Near-IR Camera overview.

	Single-channel implementation	***Dual-channel implementation***	
		Short-Wavelength Channel	Long-Wavelength Channel
Operational wavelengths	900–1950 nm	900–1338 nm	1338–1950 nm
Broad-band filters	F1075W,F1250W,F1435W F1650W	F1075W,F1250W	F1435W,F1650W
Medium-band filters	F0952M,F1020M,F1095M, F1180M,F1275M,F1386M, F1509M,F1648M,F1790M, (F1850M)	F0952M,F1020M,F1095M, F1180M,F1275M	F1400M,F1515M,F1648M, F1790M,(F1850M)
Narrow-band filters	F0956N,F1086N,F1262N, F1282N,F1290N,F1649N, F1875N,F1887N	F0956N,F1086N,F1262N, F1282N,F1290N	F1649N,F1875N,F1887N
Grisms	G1120L,G1625L	G1120L	G1625L
Exposure times	0.1 up to 2000 s	0.1 up to 2000 s	0.1 up to 2000 s
Detector technology	HgCdTe, 2k×2k	HgCdTe, 2k×2k	HgCdTe, 2k×2k
Pixel size	18 μm = 0.″0566	18 μm = 0.″0566	18 μm = 0.″0566
Instantaneous Field size	19′×15′ = 10×8 detectors	19′×15′ = 10×8 detectors	19′×15′ = 10×8 detectors
Pointing accuracy w/FSM	$<1/4$ pixel over 2000 s	$<1/4$ pixel over 2000 s	$<1/4$ pixel over 2000 s
Inter-detector gap size	∼35 pixels	∼35 pixels	∼35 pixels
Operational temperature	120 K	120 K	120 K
Full-well capacity	>250,000 e^-	>250,000 e^-	>250,000 e^-
Dark rate	<36 e^-/hr/pix	<36 e^-/hr/pix	<36 e^-/hr/pix
Read noise (rms)	<7 e^-/pix	<7 e^-/pix	<7 e^-/pix
Gain	4,8 e^-/ADU	4,8 e^-/ADU	4,8 e^-/ADU
A-to-D conversion	16-bpp	16-bpp	16-bpp
Total nr. of detectors	80	160	
Raw data volume/shot	0.671 Gigabyte	1.342 Gigabyte	
Raw data volume/24-hr	<1 Terabyte	<2 Terabyte	
Lossless compression	factor of 2–3.5	factor of 2–3.5	
Downlink volume/24-hr	<0.3–0.5 Terabyte	<0.6–1.0 Terabyte	
Mass	(tbd)	(tbd)	
Power	120–150 W	240–300 W	
Instrument lifetime	5 yr baseline, 10 yr design	5 yr baseline, 10 yr design	
Estimated Cost:	**∼120 M$**	**∼250 M$**	